AD-A168 111 LASERCOM MITIGATION PROGRAM(U) EOS TECHNOLOGIES INC 1/1
SANTA MONICA CA R E LELEVIER ET AL. 01 JUN 85
EOS-TR-50100-001 DNA-TR-85-134 DNA001-84-C-0023

UNCLASSIFIED F/G 17/2 NL

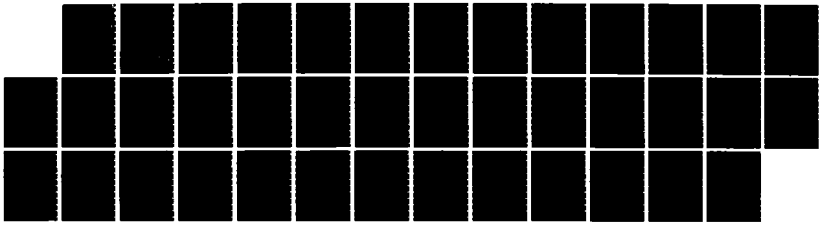

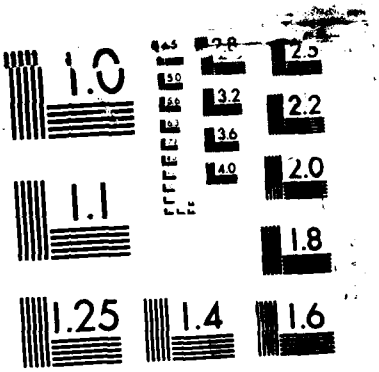

12

AD-A168 111

DNA-TR-85-134

LASERCOM MITIGATION PROGRAM

R. E. LeLevier
N. Jensen
EOS Technologies, Inc.
606 Wilshire Blvd, Suite 700
Santa Monica, CA 90401-1503

1 June 1985

Technical Report

CONTRACT No. DNA 001-84-C-0023

Approved for public release;
distribution is unlimited.

THIS WORK WAS SPONSORED BY THE DEFENSE NUCLEAR AGENCY
UNDER RDT&E RMSS CODE B322084466 S99QMXBB00048 H2590D.

DTIC FILE COPY

Prepared for
Director
DEFENSE NUCLEAR AGENCY
Washington, DC 20305-1000

86 5 5 028

UNCLASSIFIED
SECURITY CLASSIFICATION OF THIS PAGE

REPORT DOCUMENTATION PAGE

Form Approved
OMB No. 0704-0188
Exp. Date: Jun 30, 1986

1a. REPORT SECURITY CLASSIFICATION UNCLASSIFIED	1b. RESTRICTIVE MARKINGS
2a. SECURITY CLASSIFICATION AUTHORITY N/A since Unclassified	3. DISTRIBUTION/AVAILABILITY OF REPORT Approved for public release; distribution is unlimited.
2b. DECLASSIFICATION/DOWNGRADING SCHEDULE N/A since Unclassified	
4. PERFORMING ORGANIZATION REPORT NUMBER(S) EOS-TR-50100-001	5. MONITORING ORGANIZATION REPORT NUMBER(S) DNA-TR-85-134
6a. NAME OF PERFORMING ORGANIZATION EOS Technologies, Inc 6b. OFFICE SYMBOL (If applicable)	7a. NAME OF MONITORING ORGANIZATION Director Defense Nuclear Agency
6c. ADDRESS (City, State, and ZIP Code) 606 Wilshire Blvd Suite 700 Santa Monica, CA 90401-1503	7b. ADDRESS (City, State, and ZIP Code) Washington, DC 20305-1000
8a. NAME OF FUNDING/SPONSORING ORGANIZATION 8b. OFFICE SYMBOL (If applicable)	9. PROCUREMENT INSTRUMENT IDENTIFICATION NUMBER DNA 001-84-C-0023
8c. ADDRESS (City, State, and ZIP Code)	10 SOURCE OF FUNDING NUMBERS

PROGRAM ELEMENT NO	PROJECT NO	TASK NO	WORK UNIT ACCESSION NO.
62715H	S99QMXB	B	DH008656

11. TITLE (Include Security Classification)
LASERCOM MITIGATION PROGRAM

12. PERSONAL AUTHOR(S)
LeLevier, R.E. and Jensen, N.

13a TYPE OF REPORT	13b TIME COVERED	14 DATE OF REPORT (Year, Month, Day)	15 PAGE COUNT
Technical	FROM 831129 TO 841101	850601	42

16. SUPPLEMENTARY NOTATION
This work was sponsored by the Defense Nuclear Agency under RDT&E RMSS Code B322084466 S99QMXBB00048 H2590D.

17 COSATI CODES			18 SUBJECT TERMS (Continue on reverse if necessary and identify by block number)	
FIELD	GROUP	SUB-GROUP		
18	3		Laser Propagation	Soot
20	5		Turbulence	Fireball Brightness
			Smoke	Refraction

19. ABSTRACT (Continue on reverse if necessary and identify by block number)

The effects of nuclear explosions on the propagation of laser link communications systems is treated. Estimates are provided for attenuation by the smoke and soot generated by nuclear weapon induced fires for a series of laser wavelengths. Atmospheric turbulence affecting laser beam coherence is investigated, the enhanced atmospheric brightness from the visible thermal pulse of a low-altitude explosion is estimated and preliminary work on refraction effects through shock fronts is presented.

20 DISTRIBUTION/AVAILABILITY OF ABSTRACT	21 ABSTRACT SECURITY CLASSIFICATION
☐ UNCLASSIFIED/UNLIMITED ☒ SAME AS RPT ☐ DTIC USERS	UNCLASSIFIED
22a NAME OF RESPONSIBLE INDIVIDUAL Betty L. Fox	22b TELEPHONE (Include Area Code) (202) 325-7042
	22c OFFICE SYMBOL DNA/STTI

DD FORM 1473, 84 MAR 83 APR edition may be used until exhausted
All other editions are obsolete

SECURITY CLASSIFICATION OF THIS PAGE
UNCLASSIFIED

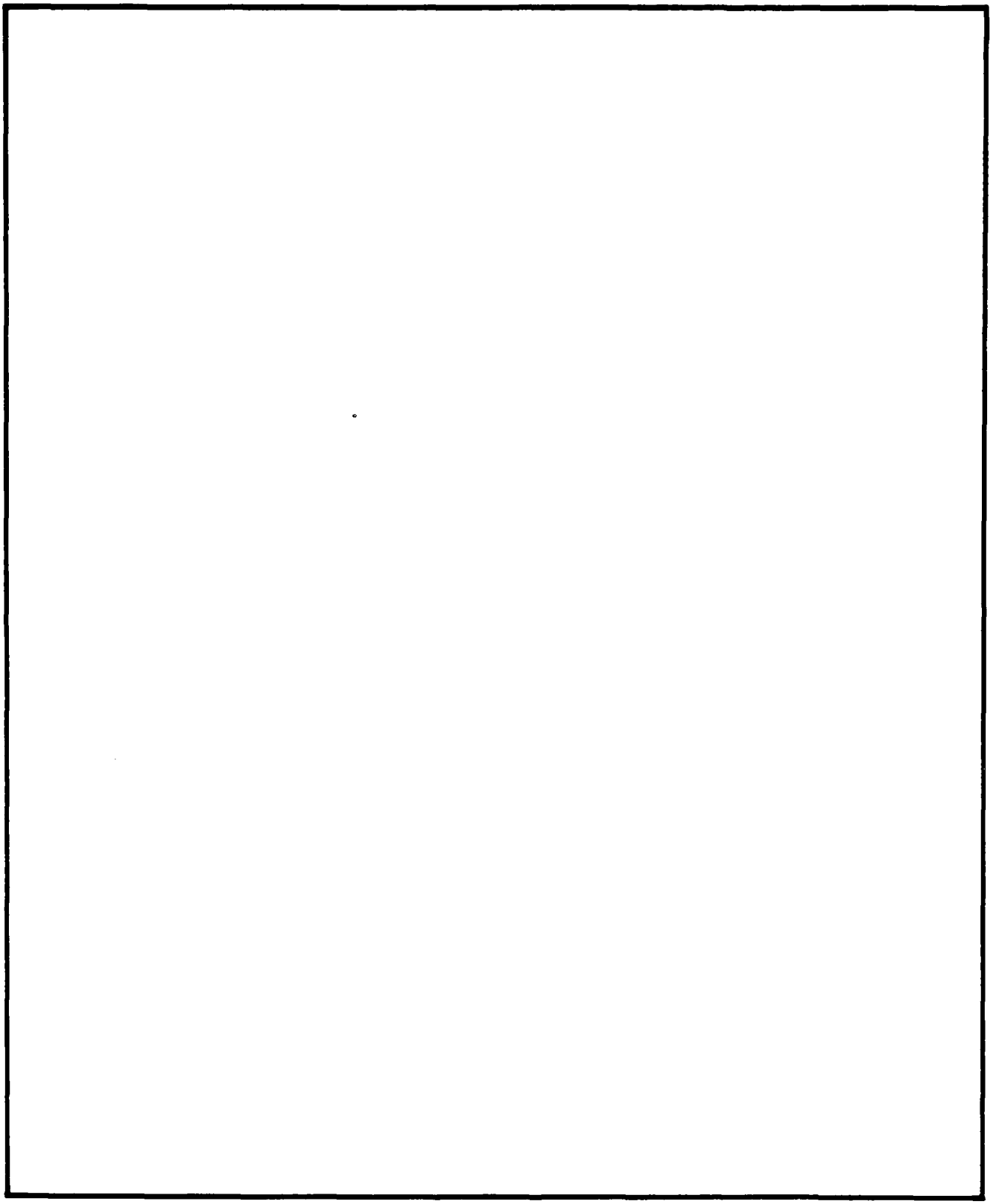

TABLE OF CONTENTS

LIST OF ILLUSTRATIONS

LIST OF TABLES

SECTION 1

INTRODUCTION

This final report covers research accomplished for the period 29 November 1983 through 1 November 1984 on DNA contract DNA 001-84-C-0023. The thrust of this activity is to identify wide-range, hundreds of kilometers in extent, nuclear weapon effects which could interfere with laser communication links from ground-based and/or aircraft-based transmitters or receivers to satellite platforms. The research concentrates on nuclear weapon bursts from the surface to altitudes up to but less than about forty-kilometer height of burst, the so-called low-altitude, mid-altitude (LAB/MAB) burst regime. Several effects have been previously identified and analyzed. These include obscuration by dust clouds generated by megaton-range surface bursts, attenuation of transmissions by smoke and soot from fires, and loss of coherence due to the atmospheric turbulence created by rising fireballs and associated winds.

This study has concentrated on three areas. One is the deflection of light beams by high-altitude shock waves. The effect appears to be potentially significant out to distances of 100 km or so. This is discussed in Section 2.1. Section 2.2 discusses the concept of coherence length with application to the case of a rising fireball (the Hill Spherical Vortex). The third area of study is the enhanced background brightness produced by scattered light from a nuclear fireball. It appears this effect is potentially significant to distances of several hundred kilometers from a nuclear detonation.

Section 3 is a brief discussion of how these effects can interfere with optical communications. Conclusions are presented in Section 4.

SECTION 2

NUCLEAR EFFECTS ON OPTICAL PROPAGATION

Nuclear detonations can, of course, affect the propagation of optical communication links in a variety of ways. The most obvious ways include absorption and scattering of light by nuclear weapon related dust, smoke and soot particles. In addition, however, there are several subtler effects that can also perturb optical propagation paths in the atmosphere. We are particularly interested in effects that extend to significant ranges (100 kilometers or more). Three such effects are as follows:

- Deflection of light beams by high-altitude shock waves.
- Increased scintillation losses resulting from increased turbulence.
- Increased background brightness caused by direct and scattered light from a nuclear fireball.

The following subsections discuss these three effects.

2.1 THE EFFECTS OF HIGH-ALTITUDE SHOCK WAVES.

The increased density of air at the front of a shock wave increases refraction of incident or exiting light rays. If the refraction is severe enough, a laser beam can be deflected out of the acceptance angle of a receiver. The magnitude of the effect depends on weapon yield, on the distance of the shock front from the point of detonation, on the altitude at which the beam encounters the shock front, and on the geometry.

Figures 1a and 1b illustrate the geometry for two cases of interest. One is the case where the laser beam enters the shock wave, transits the interior and then exits the shock. The second case is where the transmitter is suddenly inside the shock wave, and the ray "exits only." The worst case, as far as beam deflection is concerned, is at the transition point between the two cases. This can be relatively easily understood by considering the hypothetical case of a sphere with one index of refraction immersed in a medium with a different index. A light ray entering the sphere is refracted according to Snell's law, transits the sphere in a straight line, then is refracted again on exiting. The angular deflections, as the beam enters and exits, are exactly equal but opposite in sign. Thus there is a slight translation but no net deflection of the beam.

The case of a real shock wave in a real atmosphere is somewhat different. The index of refraction of the atmosphere and the shock wave both change with altitude. (The change of index with altitude causes light to bend as it propagates through a normal atmosphere.) In addition, the density of air, hence the index, follows a sort of "N" wave variation behind the shock front. Figure 2 shows a typical variation (in terms of overpressure). Because of these variations, deflections at entrance and exit to the shock wave will not be equal and opposite in sign, nor will the ray be undeflected in the interior of the shock. Thus, in general, there <u>will</u> be a net deflection.

The relative magnitude of the deflection can be qualitatively estimated. For instance, at large zenith angles (rays nearly horizontal to the ground), there is relatively little change in altitude, hence entrance and exit deflections tend to be more equal and compensate each other. For

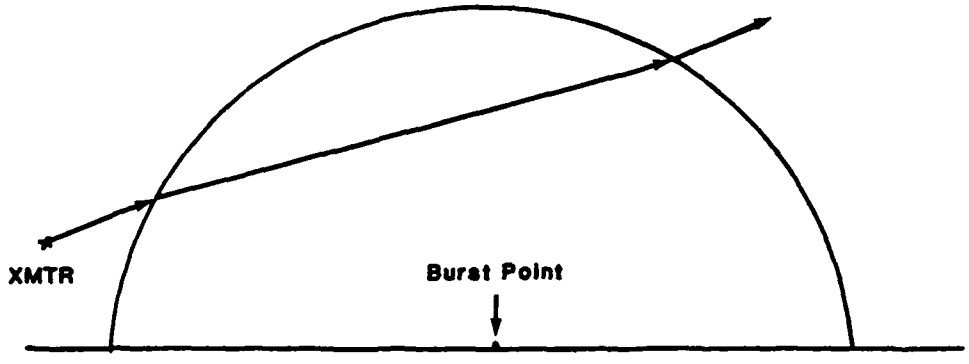

Figure 1a. Geometry for ray traversing interior of shock wave.

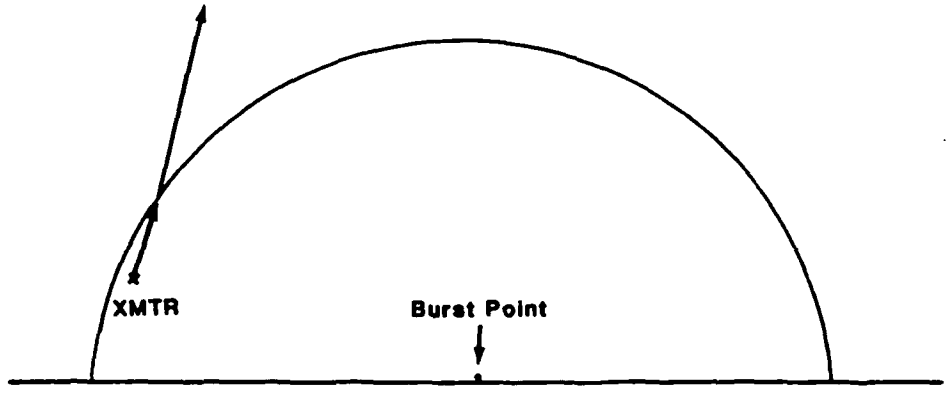

Figure 1b. Geometry for "exit only" case.

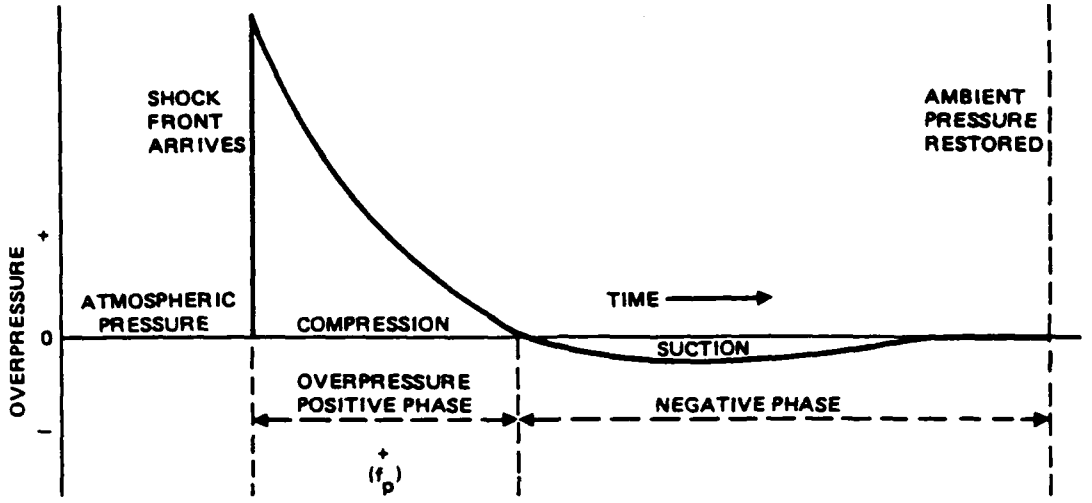

Figure 2. Variations of overpressure and dynamic pressure with time at a fixed location.

near-vertical transmission paths, on the other hand, there is a greater change in altitude between the entrance and exit points of the ray. The net deflection should therefore increase. When the ray originates within the shock, (see Figure 1b) there are no offsetting deflections and the net deflection can become large depending on the angle of incidence.

In order to calculate the net beam deflections for our two cases, we need to know how the index of refraction of air varies with altitude and how the overpressure of the shock front and "N" wave vary with weapon yield and shock radius.

2.1.1 Index of Refraction of Air.

The index of refraction of air, n, is given by

$$n = 1 + \frac{N_e q^2}{2\varepsilon_o m_e \left(\omega_o^2 - \omega^2\right)} \tag{1}$$

where N_e is the number of the electrons per unit volume, q is the electron charge, m_e is the mass of an electron, ε_o is the permittivity of free space (8.85×10^{-12} coulombs^2/newton-m^2), ω_o is the resonant frequency of the air molecules, and ω is the angular frequency of laser light of wavelength λ.

Inserting the appropriate values and constants, this can be written as

$$n = 1 + \frac{(1.66 \times 10^{-27})N}{173.3 - 1/\lambda^2} \tag{2}$$

where N is the number of molecules per cubic meter. For a standard atmosphere, N is approximately

$$N = 2.52 \times 10^{25} \, e^{-.137H} \tag{3}$$

where H is the altitude in kilometers.

2.1.2 Index of Refraction of the Shock Front and Interior.

For a contact surface burst with a single hemispherical wave, we have empirically modelled the peak overpressure, p, of the shock front as

$$p = \frac{W^{1/3}}{10R} \tag{4}$$

where W is the weapon yield in kilotons and R is the shock radius in kilometers. The density, ρ, of the air at the shock front is related to the ambient density, ρ_o, by

$$\frac{\rho}{\rho_o} = \frac{2\gamma P+(\gamma+1)p}{2\gamma P+(\gamma-1)p} \tag{5}$$

where γ is the specific heat of air and P is the ambient pressure. (1)

The length of the positive phase of the "N" wave has been empirically modeled as

$$L_+ = .03W^{1/3} \ln\left(\frac{125R}{W^{1/3}}\right). \tag{6}$$

We have initially assumed a rather simplistic model in which the density decreases linearly over this distance and continues to decrease for the same distance in the negative phase until it equals the reciprocal of the density ratio at the shock front (see Figure 3). At greater distances behind the front, it is assumed the density is the same as ambient.

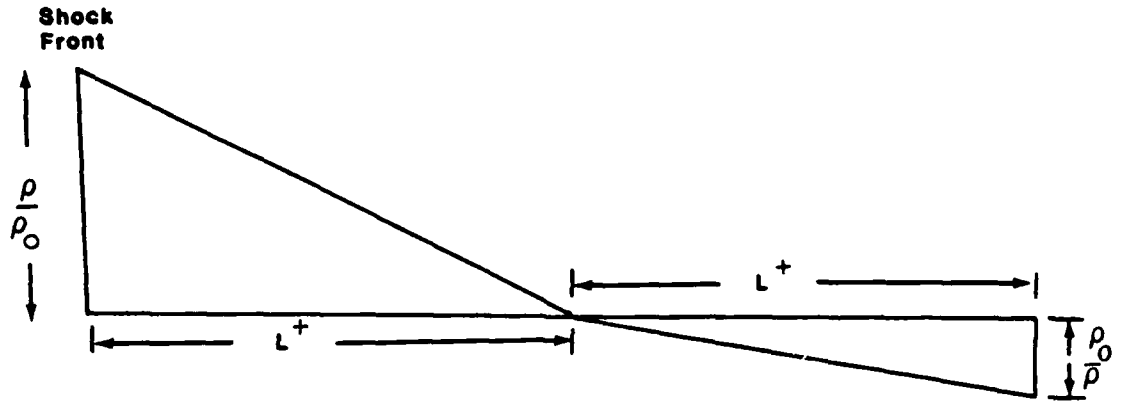

Figure 3. Simple model for density ratio behind shock front.

The indices of refraction for any point on or within the hemispherical shock wave is then found by the same method as for air. That is, the density of air molecules is determined using the above models and altitude calculations. The indices are then calculated using Equations (2 and 3).

2.1.3 Results.

Figure 4 shows the net deflections for a 1-Megaton weapon at a burst distance of 50 km (measured on the ground). The transmitters are located at altitudes of 20 and 25 km. When the zenith angle is near the transition point, i.e. where the ray is tangent to the sphere, the net deflections are relatively large (and they change sign). As the zenith angle increases or decreases, the net deflection decreases. As expected, the net deflections for a transmitter at 25-km altitude is significantly reduced compared to the 20-km case. The time duration of these deflections will generally be many seconds.

2.2 TURBULENCE EFFECTS.

Starting with the basic result of Ref. 2 for the coherence length of the atmosphere due to turbulence,

$$\ell_c = \left(\frac{\lambda^2}{4Z\ C_n^2} \right)^{3/5}, \tag{7}$$

where λ is the laser wavelength, Z is the propagation path-length through the turbulence and C_n^2 is the refractive index structure constant, we derive a scaling law which measures the strength of turbulent velocity flow which can limit the effective aperture of an optical telescope. The meaning of ℓ_c, the coherence length, is that if the turbulent flow is

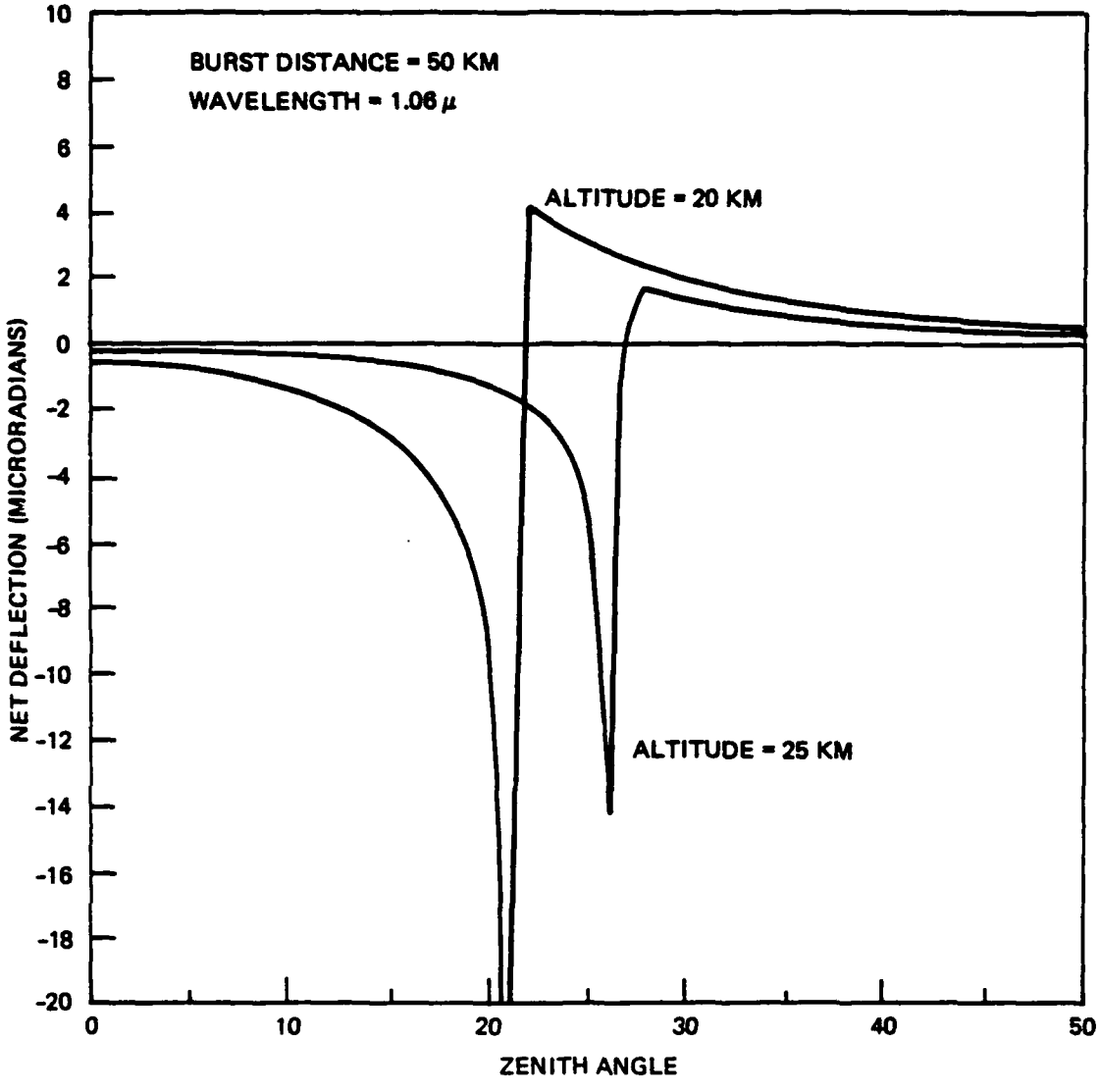

Figure 4. Net deflection vs. zenith angle for a 50-km burst distance.

strong enough so that $\ell_c < D$, where D is the telescope diameter, then the effective aperture of the telescope is limited to ℓ_c, thereby degrading the beam quality. The result is,

$$\ell_c = 1.2 \times 10^{-4} \lambda_{\mu m}^{6/5} Z_{km}^{-3/5} L_{km}^{2/5} M^{-6/5} \left(\frac{\rho}{\rho_o}\right)^{-6/5} (m), \quad (8)$$

where λ is the laser wavelength in micrometers, Z is the path length through the turbulence in kilometers, L is the outer scale of the turbulence in kilometers, M is the Mach number of turbulent eddy velocities, ρ is the air density at the altitude of the propagation path and ρ_o is the air density at sea level.

To get a feel for the numbers, let us take, $\lambda_{\mu m} = 1$, $Z_{km} = 10$, $L_{km} = 10$, $\rho/\rho_o = 3.2 \times 10^{-2}$, corresponding to an altitude of 25 km. For these values $M = 10^{-2}$, corresponding to a turbulent eddy velocity of 3 m/sec. We find, $\ell_c = 1$ m. The technical discussion presents the details of this derivation.

2.2.1 Technical Discussion.

We follow the development of Ref. 2, and consider phase fluctuations due to a turbulent eddy of dimension where,

$$\ell_o < \ell < L \quad (9)$$

ℓ_o is the inner scale of turbulence and L is the outer scale of turbulence. The phase structure function for a laser beam propagating through the turbulent eddy is,

$$<\Delta\Phi^2,\ (\ell) > = k^2\ell^2 < n'^2(\ell) > , \tag{10}$$

where, k is the wave number of the laser and n' is the fluctuation of the index of refraction due to the eddy of size ℓ.

For a locally homogeneous and isotropic turbulent medium which obeys the Kolmogoroff two-thirds law, we have,

$$<n'^2(\ell) > = C_n^2 \ell^{2/3}, \tag{11}$$

where C_n^2 is the refractive index structure constant. Thus,

$$<\Delta\Phi,^2(\ell) > = k^2\ C_n^2 \ell^{8/3},\ \ell_o > \ell > L. \tag{12}$$

Imagine that we are propagating over a path length Z in the turbulent medium. There are approximately Z/ℓ turbules over the entire path length Z. Assuming the phase differences over each turbule are uncorrelated, the total phase difference fluctuation is proportional to the number of turbules along the path and,

$$<\Delta\Phi^2\ (\ell) > = k^2\ Z\ C_n^2\ \ell^{5/3}. \tag{13}$$

Suppose ℓ_c is the largest eddy for which the beam may be considered coherent. Then from,

$$<\Delta\Phi^2(\ell_c)\ > \simeq \pi^2, \tag{14}$$

we have,

$$\ell_c = \left(\frac{\lambda^2}{4\ z\ C_n^2} \right)^{3/5}, \tag{15}$$

where λ is the wavelength of the laser beam. This is the basic result of Ref. 2.

The refractive index structure constant, C_n, is,

$$C_n^2 = < n^{-2} > / L^{2/3}, \tag{16}$$

where L is the outer scale of the turbulence. We may write,

$$< n^{-2} >^{1/2} = A \frac{\rho}{\rho_o} \frac{\delta\rho}{\rho}, \tag{17}$$

where A is the familiar constant, 3×10^{-4}, ρ_o is the sea level air density, ρ is the air density at altitude and $\delta\rho$ is the fluctuation in the air density.

For small fluctuations in the air density, it follows from the conservation equations that ρV is conserved leading to,

$$\frac{\delta\rho}{\rho} = \frac{\delta v}{c}, \tag{18}$$

where c is the speed of sound and δv is the turbulent velocity of the largest eddy. Thus,

$$C_n^2 = \frac{A^2}{L^{2/3}} \left(\frac{\rho}{\rho_o} \right)^2 \left(\frac{\delta v}{c} \right)^2 \tag{19}$$

which relates the refractive index structure constant to the altitude of the turbulent flow (through the air density ρ) and the Mach number of the turbulent flow,

$$M = \frac{\delta v}{c} \quad . \tag{20}$$

Finally, we have,

$$\ell_c = \frac{L^{2/5}}{(4\ Z)^{3/5}} \left[\frac{\lambda}{A\ \frac{\rho}{\rho_o}\ M} \right]^{6/5} , \tag{21}$$

which is the basic scaling law in this simple model which relates the coherence length to the parameters of interest. The physical meaning of this coherence length is that the effects of turbulence at altitude can change the effective aperture of an optical telescope of D to a partially coherent aperture of diameter ℓ_c, for $\ell_c < D$. We note the rather modest dependence on air density and laser wavelength. Thus, evaluating Eq. (21), we get,

$$\ell_c = 1.2 \times 10^{-4} \lambda_{\mu m}^{6/5}\ Z_{km}^{-3/5}\ L_{km}^{2/5}\ M^{-6/5} \left(\frac{\rho}{\rho_o}\right)^{-6/5} (m) . \tag{22}$$

It is instructive to inquire as to the Mach number of the turbulent flow which would limit the coherence length to a value of one meter. Typical telescope diameters of airborne optical systems are of the order of 0.5 to 1 m and so this Mach number would set a threshold on where turbulence could start to affect system performance.

From Eq. (22), setting ℓ_c equal to one meter, we find,

$$M = 5.1 \times 10^{-4}\ Z_{km}^{-1/2} \left(\frac{\rho_o}{\rho}\right) \lambda_{\mu m}\ L_{km}^{1/3} \cdot \left(\ell_c = 1m\right) . \tag{23}$$

let us take a basic set of parameters: $\lambda = 1_{\mu m}$, L = 10 km, Z = 10 km.

Using the basic set of parameters and taking the propagation path to be at 25 km altitude, we have $M = 1.0 \times 10^{-2}$. With a sound speed of 300 m/sec at an altitude of 25 km, the turbulent velocity in an eddy which would limit the coherent aperture to one meter would be $\delta v \simeq 3$ m/sec. For a propagation path of 1 km, the corresponding turbulent eddy velocity would have to be $\delta v \simeq 10$ m/sec.

Thus, in evaluating the effects of turbulent flow fields on limiting coherent apertures, we are interested in eddy velocities of only about 3 to 10 m/sec, depending on details of the laser path geometry.

These thresholds can be used in estimating the turbulent flow fields generated by rising fireballs (see Refs. 3-6). One such model, though admittedly unrealistic, is "The Hill Spherical Vortes". This model is discussed in the following subsection.

2.2.2 The Hill Spherical Vortex.

The Hill sperical Vortex has the virtue that it is simple, is described by a set of complete equations, but has nothing to do with the physics of real fireballs in the atmosphere. As discussed in Ref. 4, the vortex moves through a uniform, incompressible fluid with constant velocity, with no

entrainment and with no external forces acting. All these approximations are invalid for the case of interest but it is still the only description of a vortex available which is easy to work with (Ref. 4).

We were curious as to the implications of the external flow field behavior on the coherence length discussed in the previous section.

The magnitude of the external flow field of the vortex is, (8)

$$V = U \frac{a^3}{r^3} \left(1 - 2 \sin^2\theta + \frac{5}{4} \sin^4\theta\right)^{1/2} \tag{24}$$

where U is the speed of the vortex, "a" the radius, "r" the radial distance from the vortex center and θ is the polar angle measured from the axis of the direction of motion (8). At $\theta = \pi/2$, the waist of the vortex,

$$V = \frac{1}{2} U \frac{a^3}{r^3} . \tag{25}$$

This flow, of course, is laminar. However, if there were some mechanism that caused the flow to become turbulent, we would like to look at the implications on the coherence length. Inserting V into Eq. (8) for the coherence length, we find,

$$\ell_c \sim U^{-6/5} r^{3.6}, \tag{26}$$

indicating that the presumed influence of turbulence on distance from the vortex decreases very rapidly, measured in distances like a fireball radius or so. It will be interesting to see what a more realistic fireball turbulence model will predict.

2.3 ENHANCED BACKGROUND BRIGHTNESS.

For downward-looking optical systems, scattered in-band sunlight from clouds or snow can increase the noise levels in a receiver. Light from a nuclear detonation can similarly increase receiver noise levels. The effect is highly dependent on weather and geometry (among other things), but it appears the effect could be significant out to ranges of 100 kilometers or so.

In order to simplify calculations and, at the same time, make them more meaningful, it was decided to calculate the distance at which the attenuated light from a fireball is roughly equal to that of the sun. In a crude way, this should approximate the area over which the background noise could be at least twice as bad as for normal sunlit conditions.

2.3.1 Technical Discussion.

When a nuclear weapon detonates in the atmosphere, a great deal of its energy is emitted in the form of visible light. When this light propagates through the atmosphere, it is scattered and can create an enhanced background for sensors looking through or at the atmosphere. The magnitude and extent of this enhanced background will depend primarily on the weapon yield, its height-of-burst, and weather conditions. The effect on any given sensor will depend on geometry, its field-of-view, and its spectral sensitivity. The following is an initial analysis of this phenomena.

The amount of radiated light from a nuclear weapon and its spectral distribution depend on how the fireball size and temperature change with time. The radius increases rapidly in the first second or so as shown in Figure 5 (1).

The temperature of the fireball has a time profile similar to that shown in Figure 6 (1). For a 20-KT weapon, the "observed" temperature reaches a maximum of about 9000°K in less than a millisecond, drops to about 2000°K at 10 milliseconds, and then again rises to about 8000°K at .2 seconds before beginning a steady decay.

An estimate of how the fireball radius varies with time and yield was made by curve-fitting Figure 5. This gives

$$R_B = [779 + 229 \log t] \left(\frac{W}{20}\right)^{.4} \qquad (27)$$

where R_B is the fireball radius in feet, t is the time in seconds, and W is the weapon yield in kilotons.

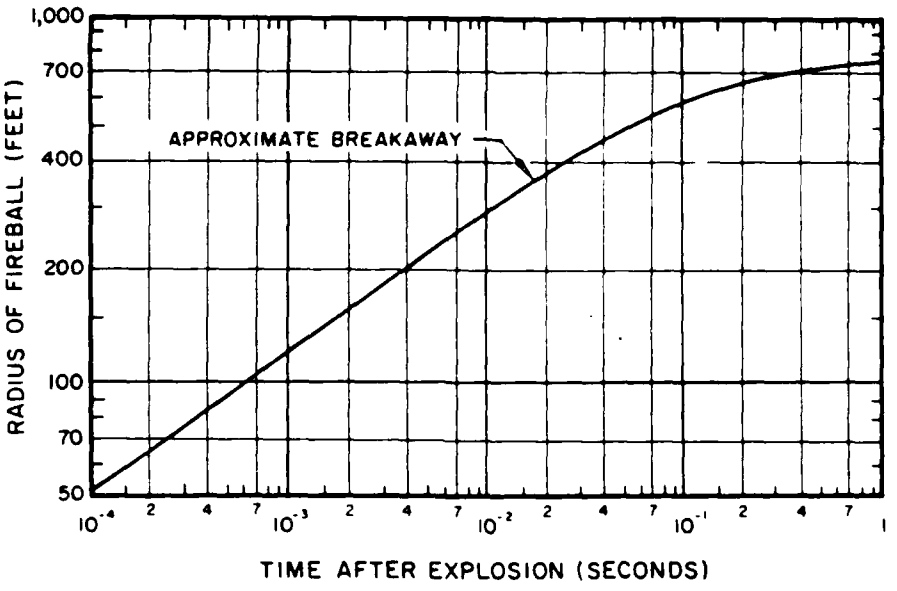

Figure 5. Variation of fireball radius with time in a 20-kiloton explosion. (From Ref. 1)

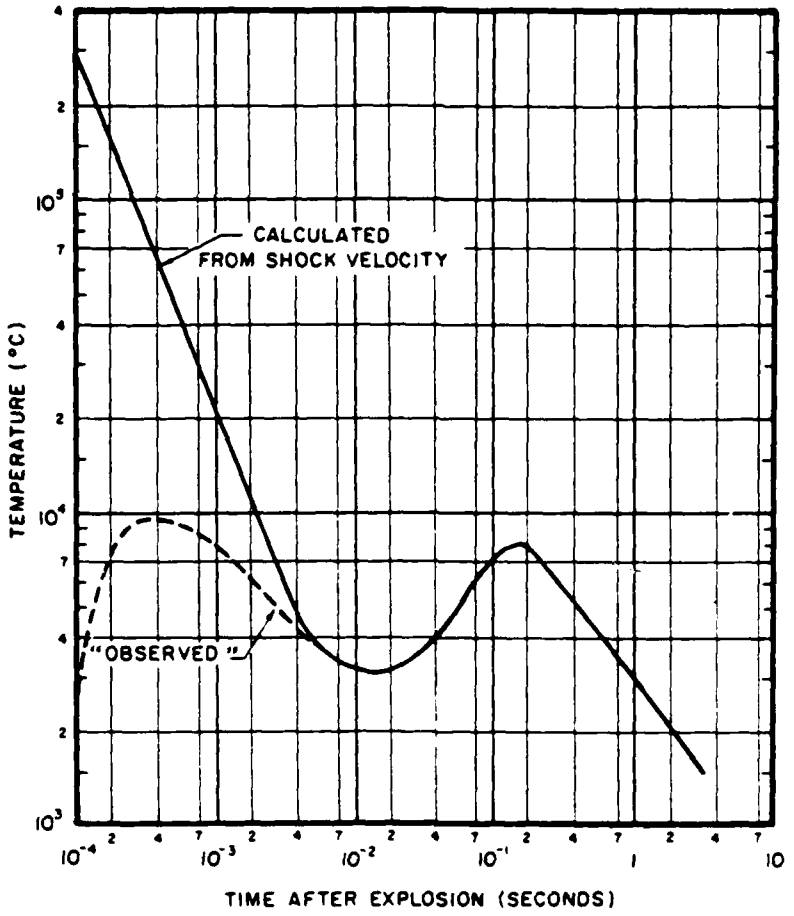

Figure 6. Variation of apparent fireball surface temperature with time in a 20-kiloton explosion. (From Ref. 1)

Similar temperature-time relations were developed by curve-fitting Figure 6. The results were

$$\log T = 4.3238 + .602 \log(t), \quad .02 \le t \le .2 \text{ sec, and}$$
$$\log T = 3.4822 - .602 \log(t), \quad .2 \le t \le 2 \text{ sec.} \qquad (28)$$

Using the above relations, the amount of radiation at a particular wavelength can be calculated as function of time and distance from the fireball.

For a blackbody at a temperature T, the spectral radiation per unit area and per unit wavelength, W_λ is given by

$$W_\lambda = \frac{A}{\lambda^5} \quad \frac{1}{e^{B/\lambda T}-1} \tag{29}$$

where λ is the wavelength and A and B are constants. The spectral radiation per unit area as a function of range can be found by multiplying this expression by the area of the fireball (as a function of time) and dividing by the area of a sphere with a radius equal to the range.

The range at which the light from a weapon would equal the effect of scattered sunlight is given by

$$R = R_B \frac{R_{se}}{R_s} \left\{ \frac{e^{1.4388/\lambda T}-1}{e^{1.4388/.59\lambda}-1} \right\}^{1/2} e^{-\alpha R/2} \tag{30}$$

where R is the range, λ is the wavelength, T is the fireball temperature (the temperature of sun is taken to be 5900°K), R_{se}/R_s is the ratio of the sun's distance to its radius, and the atmospheric attenuation of the weapon radiation is accounted for by the $e^{-\alpha R/2}$ term.

The atmospheric attenuation becomes important at some wavelengths. Table 1 shows the attenuation coefficients that were used for each wavelength. They represent combined molecular and aerosol scattering and absorption for clear, mid-latitude, summer conditions at an altitude of 4-5 kilometers.

Table 1. Attenuation coefficients for selected wavelengths. Clear, mid-latitude, summer, 4-5 km altitude. (From Ref. 9)

WAVELENGTH (microns)	ATTENUATION COEFFICIENT (/km)
.515	.102
.86	.0052
1.06	.0038
10.6	.056

2.3.2 Results.

Figure 7 shows computer printouts indicating how fireball temperature and radius vary with time for a 20-KT and 1-MT weapon and a 1.06 micron wavelength. Figures 8 and 9 show how the "effective" range vs. time varies with wavelength for the two weapon yields.

These calculations indicate that a small (20-KT) weapon may have a significant effect on atmospheric brightness out to a range of about 50 km. A 1-MT weapon could have an effect to ranges in excess of 200 km. The time durations are relatively short (compared to a shock wave, for instance), but they are sufficient to cause problems with high-data-rate transmission systems.

Because of the variation of attenuation coefficients with altitude, the range of the effect will also vary with altitude. Figure 10 illustrates this for a wavelength of 1.06 microns and a 1-MT weapon. (The values of the attenuation coefficients are given in Table 2.) There is a strong dependence for altitudes below 25 km.

********** WEAPON/SOLAR CALCULATIONS **********

WAVELENGTH= 1.06 YIELD (KT)= 20 ATTENUATION (/KM)= .0038

TIME MILLISEC	TEMPERATURE (K)	FIREBALL (FT)	RANGE (KM)
20	2273	390	4
38	3216	454	11
56	3990	492	17
74	4669	520	23
92	5285	542	29
110	5854	559	34
128	6387	575	39
146	6891	588	43
164	7371	599	47
182	7830	610	50
200	8272	619	54
380	5708	683	40
560	4576	721	31
740	3912	749	25
920	3465	771	21
1100	3139	788	17
1280	2889	804	15
1460	2690	817	13
1640	2527	828	11
1820	2390	839	9
2000	2273	848	8

********** WEAPON/SOLAR CALCULATIONS **********

WAVELENGTH= 1.06 YIELD (KT)= 1000 ATTENUATION (/KM)= .0038

TIME MILLISEC	TEMPERATURE (K)	FIREBALL (FT)	RANGE (KM)
20	2273	1865	18
38	3216	2170	47
56	3990	2354	74
74	4669	2487	97
92	5285	2590	117
110	5854	2675	134
128	6387	2747	149
146	6891	2810	163
164	7371	2865	175
182	7830	2915	186
200	8272	2960	196
380	5708	3265	153
560	4576	3449	124
740	3912	3582	103
920	3465	3685	87
1100	3139	3770	74
1280	2889	3842	64
1460	2690	3905	55
1640	2527	3960	48
1820	2390	4010	42
2000	2273	4055	37

Figure 7. Printouts showing fireball temperature and radius as a function of time.

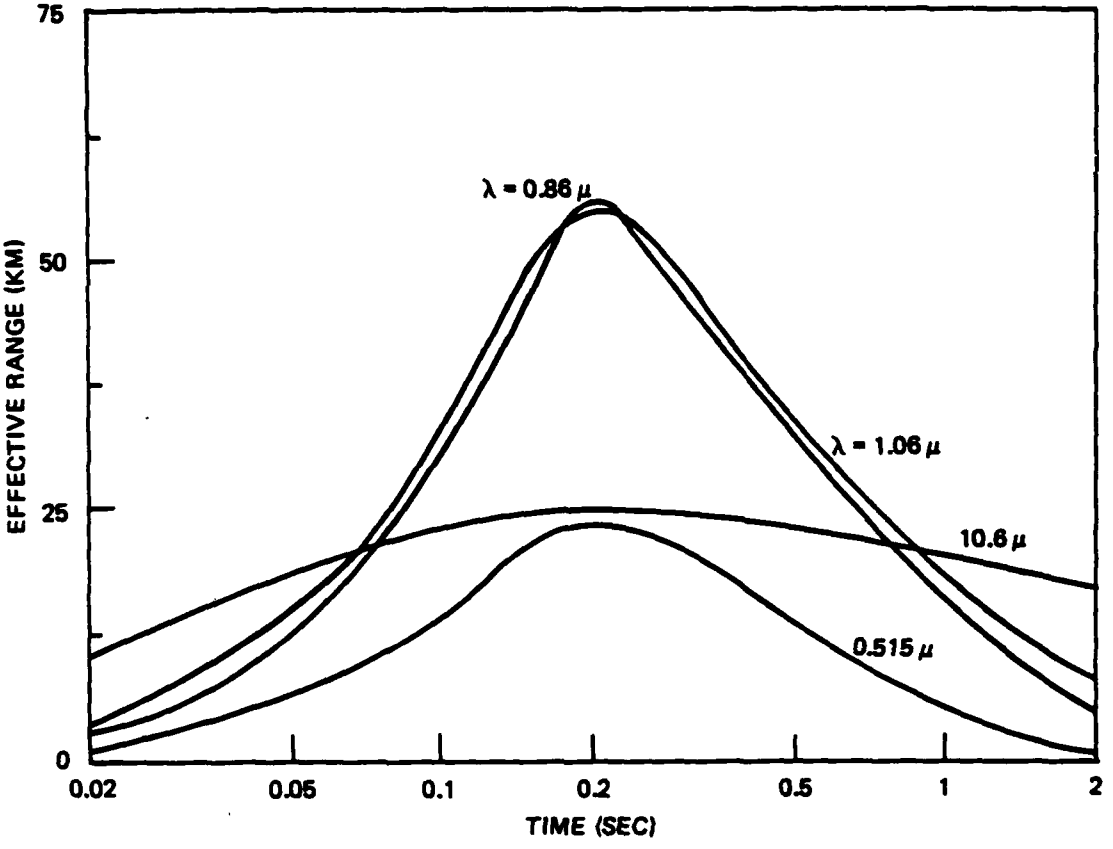

Figure 8. Effective range vs. time for selected wavelengths and a 20-KT weapon.

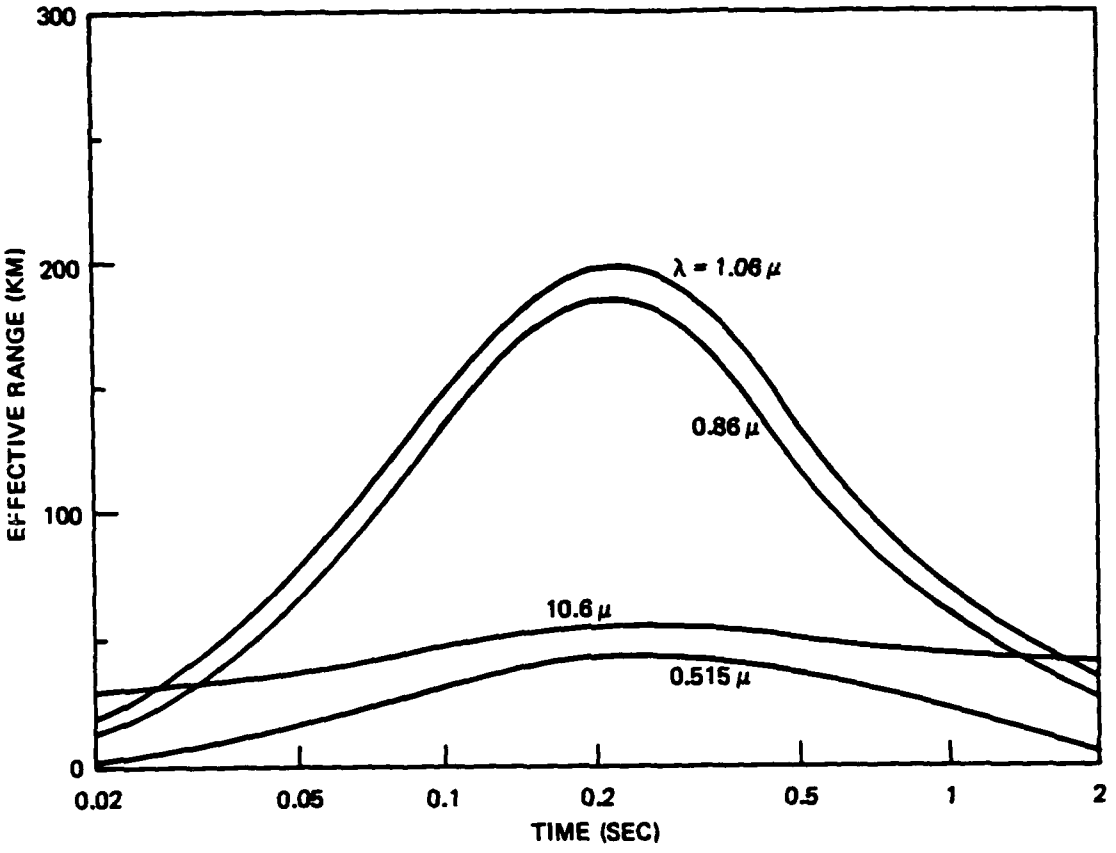

Figure 9. Effective range vs. time for selected wavelengths and a 1-MT weapon.

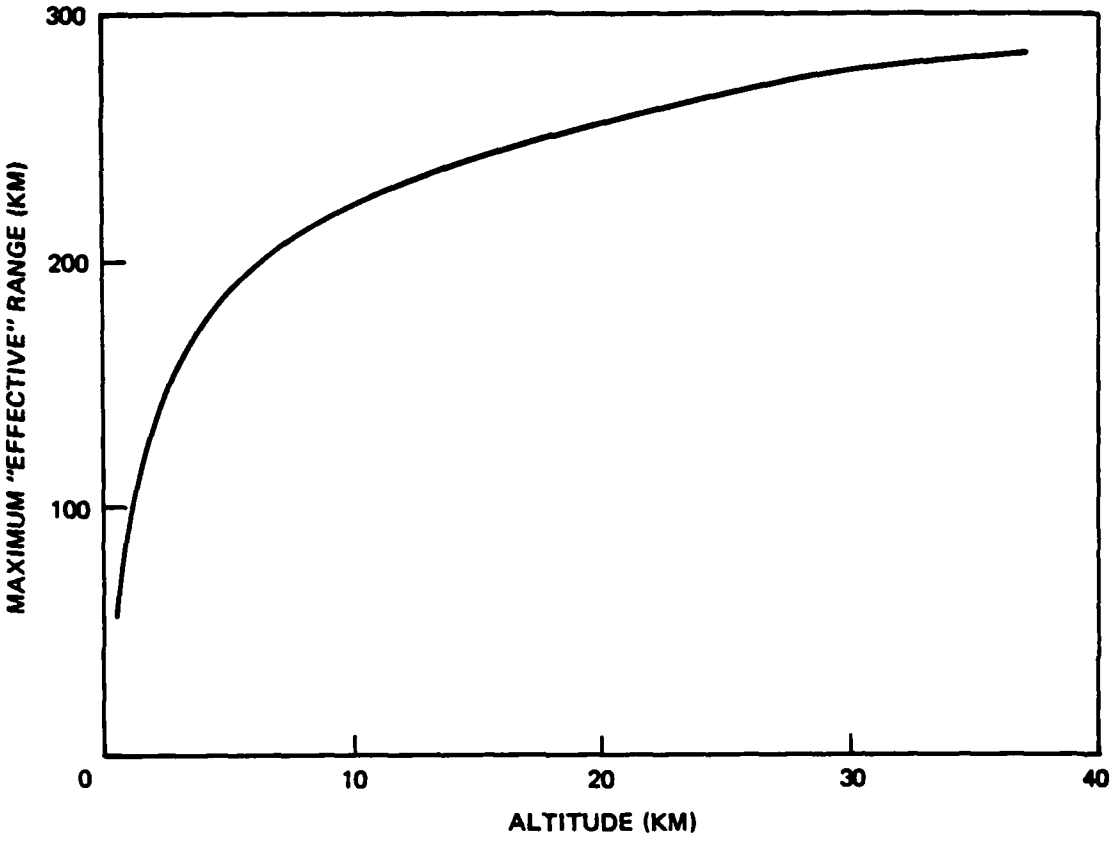

Figure 10. Maximum effective range vs. altitude for 1-MT weapon and 1.06μ wavelength (clear, summer, mid-latitude conditions).

Table 2. Attenuation coefficient as a function of altitude for 1.06 microns. Clear, summer, mid-latitude. (From Ref. 9)

ALTITUDE (km)	ATTENUATION COEFFICIENT (/km)
0-1	.062
4-5	.0038
9-10	.0021
14-15	.00172
19-20	.00088
24-25	.00026
30-35	.000048
35-40	.000015

SECTION 3

WARTIME EFFECTS ON OPTICAL COMMUNICATIONS LINKS

In general, optical communications are more robust than conventional communications. However, there are several nuclear effects that may uniquely affect optical propagation and optical noise levels as discussed in Section 2.

For example, it appears, from the analysis in Section 2.1, that high-altitude shock waves can cause substantial deflections of optical links over large areas. The deflections can last for seconds and result in loss of data and perhaps a break in the link lock. It is worth noting also that these results are based on a symmetrical, smoothly varying model. If the shock wave is not perfectly spherical, or if atmospheric density does not vary perfectly smoothly with altitude, the deflections will generally be worse. The shock waves from nearby, multiple detonations can also merge to create a surface of increased density difference (hence more severe deflections).

Another example is the increased optical noise created when the atmosphere scatters light from a nuclear fireball. It appears that the effect is roughly equivalent to that from scattered sunlight at ranges in excess of 200 kilometers (for a 1-MT weapon). If the scattered light were in the field-of-view of a receiver, it could lead to increased noise levels and the possible loss of data. (The effect can last for approximately a second.) An accurate estimate of the effect in a given situation would depend not only on the geometry, wavelength, and "normal" background but also on design details such as filtering, polarization, data rate, etc. However, it is also possible that the enhanced background can combine with other effects from shock waves and

turbulence to degrade signal-to-noise ratios further. Because the time duration of the optical background effect is on the order of a second, multiple bursts would have no combined effect unless they occurred in less than a second. If, however, multiple detonations are nearly simultaneous, the combined effect at a given point in the atmosphere is just the sum of the scattered light intensities for the appropriate times and distances.

Turbulence also has an effect on optical propagation. As discussed in Section 2.2, a useful way to describe the effect is in terms of coherence length. If, for instance, the coherence length of the turbulence is .1 meters, then this is roughly the maximum useful size for an aperture transmitting through turbulence. (The effect will be different for transmitting and receiving apertures depending on the relative distance between the platform and the turbulent media.)

A nuclear detonation creates turbulence in a number of ways. The rising fireball itself creates an updraft with inflowing winds. The traveling shock wave and the pressure gradients behind it also generate winds. Fires will also create winds. In the case of multiple bursts, some analyses indicate that hurricane-level winds may be created and persist for hours and even days. Thus it is quite possible that turbulence effects can be widespread and long-lasting. The effect on a particular link will depend on the altitude at which the propagating beam encounters the turbulence. The lower the altitude, the more severe the degradation, of course.

Table 3 lists these optical effects. The time duration of the effects range from very short (1 sec) for enhanced optical backgrounds to many hours or days for

dust/soot obscurations and turbulence. The spatial extent of the effects are generally hundreds of kilometers.

Of course the probability that a particular system might be affected depends on more than the time duration and spatial extent of an effect or set of effects. Links that do not propagate through the atmosphere are less subject to interference. The altitude, pointing angles, and field-of-view of transmitter/receivers make a difference. Weather and backgrounds (snow, clouds, etc.) are also factors.

Table 3. Summary of nuclear effects on optical communication links.

EFFECT	SPATIAL EXTENT	TIME DURATION	COMMENTS
DUST/SOOT	100's of Km	Days	Increases Transmission Losses
HIGH-ALTITUDE SHOCK WAVES	> 50 Km Radius	Seconds	Deflects Beams Propagating Across Shock Wave
TURBULENCE	Large	Hours-Days	Multibursts can Create Extensive, Persisting Areas of Wind Turbulence
ENHANCED OPTICAL BACKGROUNDS	50-300 Km Radius	< 1 sec	Increases Optical Noise in Receivers

SECTION 4

CONCLUSIONS

Although optical communications systems are generally less subject to damage from nuclear effects than conventional microwave or high frequency radiowave communications, the threat of interference is still substantial. There is also the strong possibility that combinations of effects apply. For instance, turbulence, shock waves, and enhanced optical backgrounds could all affect a particular link simultaneously (although the durations of the effects differ).

When we consider the phenomena that uniquely interfere with optical communications, it appears that their spatial extent is large enough so that they cannot be ignored. However, they do not cause permanent damage. The most likely prospect is that data would be lost for a few seconds, although it is also possible that lock could be broken. The reason for this is that the beam width of typical laser communications links are quite narrow, of the order of a microradian, and it does not take much beam deflection to break a synchronized link. Finally, the models that have been used in these analyses are by intent, fairly simple and quite crude. Some straightforward changes could make substantial differences.

We would not expect a shock wave to be perfectly spherical because of variations in the speed of sound with altitude. Consequently, net deflections are likely to be more severe than those predicted by the simple spherical model. An examination of non-spherical shocks with local turbulence is an important topic for further study.

We find significant distortion effects at very modest levels of turbulent velocity flow fields, a few meters

per second. There are two aspects of turbulent flow associated with LAB/MAB bursts that warrant further study. One is the direct generation of turbulent flow fields due to the rise and stabilization of the fireball vortex itself. The extent, strength and persistence of these flow fields is important to understand. A second aspect of turbulence has to do with the turbulence of the normal ambient atmosphere and the ambient wind shears at altitude. The reason this could be important is in connection with the beam refraction by shock waves discussed above. Since refraction effects are significant at long ranges where the shock wave is sonic, ambient turbulence and wind shear could distort the sonic shock front and exacerbate the refraction effects.

SECTION 5

LIST OF REFERENCES

1. S. Glasstone, The Effects of Nuclear Weapons, U.S. Government Printing Office, Rev. Ed. February 1964.

2. Tio, T.K., et al., Continuous-Wave Laser Beam Propagation in the Atmosphere, RDA-TR-116011-002, October 1981.

3. Ionospheric Effects and Energy Loss from the Blast Wave from Low-Altitude Nuclear Bursts, DNA 3494T, MRC, 17 December 1974.

4. Implications of Vortex Theory for Fireball Motion, DNA 3581F, 6 March 1974, MRC.

5. Ionospheric Gravity Waves from Nuclear Surface Bursts, ARPA, MRC-R-825, 15 March 1984.

6. A Model for Gravity Waves Produced by Low-Altitude Explosions for Use In Communications Studies, DNA 588T, 1 September 1981, MRC.

7. Wittwer, L., Radiowave Propagation in Structured Ionization for Satellite Applications, DNA 5304D, December 1979.

8. Lamb, Sir Horace, Hydrodynamics, Dover Publications, April 1932, p 244.

9. McClatehey, R.A., et al., "Optical Properties of the Atmosphere," Handbook of Optics, ed. W. Driscol and W. Vaughan.

DISTRIBUTION LIST

DEPARTMENT OF DEFENSE

DEFENSE INTELLIGENCE AGENCY
ATTN: RTS-2B

DEFENSE NUCLEAR AGENCY
ATTN: RAAE
ATTN: RAAE K SCHWARTZ
ATTN: RAEE P LUNN
ATTN: STNA
4 CYS ATTN: STTI/CA

DEFENSE TECHNICAL INFORMATION CENTER
12 CYS ATTN: DD

DEPARTMENT OF ENERGY

SANDIA NATIONAL LABORATORIES
ATTN: D DAHLGREN
ATTN: ORG 1231 R C BACKSTROM
ATTN: ORG 1250 W BROWN
ATTN: ORG 4231 T WRIGHT

OTHER GOVERNMENT

CENTRAL INTELLIGENCE AGENCY
ATTN: OSWR/NED
ATTN: OSWR/SSD FOR K FEUERPFETL

DEPARTMENT OF DEFENSE CONTRACTORS

BERKELEY RESEARCH ASSOCIATES, INC
ATTN: C PRETTIE
ATTN: J WORKMAN
ATTN: S BRECHT

EOS TECHNOLOGIES, INC
ATTN: B GABBARD
2 CYS ATTN: N JENSEN
2 CYS ATTN: R LELEVIER

JAYCOR
ATTN: J SPERLING

KAMAN TEMPO
ATTN: DASIAC

KAMAN TEMPO
ATTN: B GAMBILL
ATTN: DASIAC
ATTN: W MCNAMARA

MAXIM TECHNOLOGIES, INC
ATTN: E TSUI
ATTN: J MARSHALL
ATTN: R MORGANSTERN

MISSION RESEARCH CORP
ATTN: F GUIFLIANO
ATTN: G MCCARTOR
ATTN: TECH LIBRARY

PACIFIC-SIERRA RESEARCH CORP
ATTN: H BRODE, CHAIRMAN SAGE

R & D ASSOCIATES
ATTN: P HAAS

END

DTIC

7-86